

Chromium Corroles in Four Oxidation States

Alexandre E. Meier-Callahan,[†] Angel J. Di Bilio,[†] Liliya Simkhovich,[‡] Atif Mahammed,[‡] Israel Goldberg,^{*,§} Harry B. Gray,^{*,†} and Zeev Gross^{*,‡}

Beckman Institute, California Institute of Technology, Pasadena, California 91125, Department of Chemistry and Institute of Catalysis Science and Technology, Technion-Israel Institute of Technology, Haifa 32000, Israel, and School of Chemistry, Tel Aviv University, Tel Aviv 69978, Israel

Received July 9, 2001

We have isolated and characterized chromium complexes of 5,10,15-tris(pentafluorophenyl)corrole [(tpfc)H₃] (**1**) in four oxidation states: [(tpfc[•])CrO][SbCl₆] (**6**); [(tpfc)CrO] (**2**); [(tpfc)CrO][Cp₂Co] (**4**); and [(tpfc)Cr(py)₂] (**3**). Complex **6** was prepared both by electrochemical and chemical oxidation of **2**; its formulation as a Cr^{VO} ligand–radical species is based on UV–visible absorption as well as EPR measurements. Cobaltocene reduction of **2** gave **4**; it was identified as a diamagnetic d² Cr^{IV}O complex from its sharp ¹H NMR spectrum. Reaction of **2** with triphenylphosphine yielded a chromium(III) corrole, [(tpfc)Cr(OPPh₃)₂] (**5**). Owing to its air sensitivity, **5** could not be isolated in the absence of excess OPPh₃. The structure of the Cr^{III} bis-pyridine complex (**3**) was determined by X-ray crystallography (Cr–N distances: 1.926–1.952 Å, pyrrole; 2.109, 2.129 Å, pyridine).

Introduction

We have previously reported the facile synthesis of H₃(tpfc) (**1**) and the utilization of its metal complexes as catalysts for the activation of hydrocarbons.^{1,2} Air-stable and fully characterized coordination complexes of **1** include [(tpfc)CrO] (**2**),³ [(tpfc)MnBr],⁴ and [(tpfc)FeCl].⁵ The stability of Cr^V, Mn^{IV}, and Fe^{IV} corroles is in quite sharp contrast to the situation with porphyrins and related macrocycles where lower oxidation states are more common. Furthermore, our finding of spontaneous oxidation of chromium and iron corroles to Cr^{VO} and Fe^{IV}Cl states during synthesis suggests that their M^{III} complexes could be employed for dioxygen activation. Indeed, it has been shown that iron(III) complexes of **1** and other corroles oxidize in air,^{5,6} but formation of inert Fe^{IV} μ -oxo complexes limits the potential of these molecules as oxygenation catalysts.⁷

The investigations described herein centered on chromium, as only Cr^{VO} corroles have been fully characterized to date^{3,8,9} (a report of chromium(III) corroles¹⁰ has been questioned¹¹).

We have shown that **2** can transfer atomic oxygen to PPh₃ in aerobic solution to form the first authentic chromium(III) corrole, [(tpfc)Cr(OPPh₃)₂](**5**). In the absence of potential ligands, **5** is readily reoxidized to **2** by dioxygen. Reaction of **5** with pyridine gives [(tpfc)Cr(py)₂] (**3**), which has been structurally characterized. All in all, we have isolated and characterized complexes of **1** in four oxidation states: **2**, [(tpfc)CrO][−] (**4**), **3**, and [(tpfc[•])CrO]⁺ (**6**) (Scheme 1).

Experimental Section

All chemicals were obtained from either Aldrich or EM Science (solvents) and used as received, except for OPPh₃ and PPh₃, which were recrystallized before use. Tetrabutylammonium hexafluorophosphate was recrystallized from ethanol/ether. The ligand (tpfc)H₃ (**1**) was prepared according to literature procedures.² The oxidant dioxinium hexachloroantimonate (**7**) was prepared by a standard method.¹² Cobaltocene was sublimed before use.

[(tpfc)CrO] (**2**). Compound **1** (60 mg, 75.37 μ mol) was dissolved in about 20 mL of pyridine, and the solution was heated to reflux under argon. A small amount of CrCl₂ (very air-sensitive!) was added to the hot solution, and the reaction was continued until TLC examination (silica, *n*-hexane/CH₂Cl₂ = 2:1) indicated the disappearance of the starting material (about 2 h, a new green spot was obtained above the spot of corrole; if the reaction is not complete, an additional portion of CrCl₂ can be added). Once **1** was completely consumed, the solvent was evaporated, and the solid material was dissolved in CH₂Cl₂ and filtered to remove inorganic salts. A 3 g portion of silica gel was added to the filtrate, and the solvent was evaporated. Purification of the product was performed by column chromatography on silica gel, with a 22:3 mixture of *n*-hexane and CH₂Cl₂. The resulting red complex was recrystallized from CH₂Cl₂ and *n*-hexane. The yield from several such reactions was 35–38 mg (54–59%). MS (+DCI) *m/z* (% intensity): 861.9 (100%) [MH⁺]. (−DCI) *m/z* (% intensity): 861.9 (100%) [M[−]]. UV–vis (CH₂Cl₂) λ_{\max} [nm] ($\epsilon \times 10^{-3}$ [M^{−1}cm^{−1}]): 402 (81.3), 556 (14.0).

[†] California Institute of Technology.

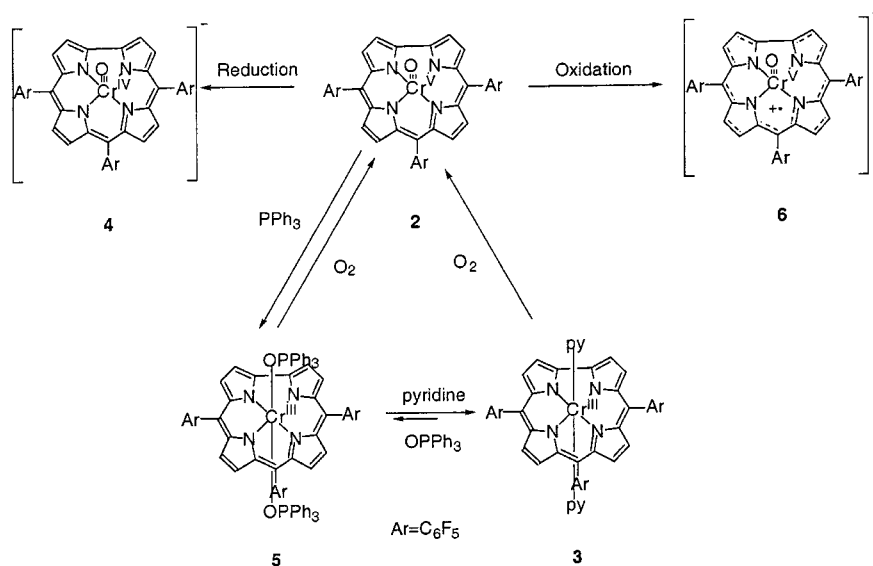
[‡] Technion-Israel Institute of Technology.

[§] Tel Aviv University.

- Gross, Z.; Simkhovich, L.; Galili, N. *J. Chem. Soc., Chem. Commun.* **1999**, 599.
- Gross, Z.; Galili, N.; Saltsman, I. *Angew. Chem., Int. Ed.* **1999**, *38*, 1427.
- Meier-Callahan, A. E.; Gray, H. B.; Gross, Z. *Inorg. Chem.* **2000**, *39*, 3605.
- Golubkov, G.; Bendix, J.; Gray, H. B.; Mahammed, A.; Goldberg, I.; Di Bilio, A. J.; Gross, Z. *Angew. Chem., Int. Ed.* **2001**, *40*, 2132.
- Simkhovich, L.; Galili, N.; Saltsman, I.; Goldberg, I.; Gross, Z. *Inorg. Chem.* **2000**, *39*, 2704.
- Vogel, E.; Will, S.; Tilling, A. S.; Neumann, L.; Lex, J.; Bill, E.; Trautwein, A. X.; Wieghardt, K. *Angew. Chem., Int. Ed. Engl.* **1994**, *33*, 731.
- Simkhovich, L.; Mahammed, A.; Goldberg, I.; Gross, Z. *Chem. Eur. J.* **2001**, *7*, 1041.
- Matsuda, Y.; Yamada, S.; Murakami, Y. *Inorg. Chim. Acta* **1980**, *44*, L309.
- Murakami, Y.; Matsuda, Y.; Yamada, S. *J. Chem. Soc., Dalton Trans.* **1981**, 855.
- Boschi, T.; Licoccia, S.; Paolesse, R.; Tagliatesta, P.; Tehran, M. A.; Pelizzi, G.; Vitali, F. *J. Chem. Soc., Dalton Trans.* **1990**, 463.

- Erlen, C.; Will, S.; Kadish, K. M. In *The Porphyrin Handbook*; Kadish, K. M., Smith, K. M., Guillard, R., Eds.; Academic Press: New York, 2000; Vol. 2, p 233.
- Barzilay, C. M.; Sibilia, S. A.; Spiro, T. G.; Gross, Z. *Chem. Eur. J.* **1995**, *1*, 222.

Scheme 1



[(**tpfc**)Cr(**py**)₂] (**3**). Metal insertion into **1** was performed as described, but at the end, the solid material was dissolved in a 9:1 mixture of benzene and pyridine and filtered. A 3 g portion of silica gel was added to the solution, and the solvents were evaporated. Purification of the product was performed by column chromatography on silica gel, with a 50:5:1 mixture of *n*-hexane/CH₂Cl₂/pyridine as eluent. The isolated green material was recrystallized from a mixture of benzene and *n*-heptane that also contained a few drops of pyridine. The yield from several such reactions was 49–53 mg (65–70%). Elemental analysis: found (calcd) for C₄₇H₁₈CrF₁₅N₆: C, 56.32% (56.25%); H, 2.07% (1.81%); N, 8.14% (8.37%). MS (+DCI) *m/z* (% intensity): 925.0 (100%) [MH⁺ – (py)], 846.0 (18%) [MH⁺ – 2(py)]. (–DCI) *m/z* (% intensity): 844.9 (100%) [M[–] – 2(py)]. UV–vis (9:1 benzene/pyridine) λ_{max} [nm] (ε × 10^{–3} [M^{–1} cm^{–1}]): 418 (33.7), 433 (38.9), 482 (23.5), 610 (12.9), 642 (14.0). ¹⁹F NMR (188 MHz) (C₆D₆, δ in ppm): –133.1, –138.8 (br s, br s, 6F, *ortho*-F), –154.8 (s, 1F, *para*-F), –155.3 (s, 2F, *para*-F), –161.8 (s, 6F, *meta*-F).

Compound **3** also was prepared from **2** by dissolving the latter (8.1 mg, 11.6 μmol) in 25 mL of CH₂Cl₂/pyridine (9:1) in the presence of excess PPh₃ (50 mg, 191 μmol). Stirring of the solution for several hours (the color changes from red to dark green), followed by solvent evaporation, yielded a residue that was dissolved in hexane/CH₂Cl₂/pyridine (220:30:2) and eluted through silica gel with the same solution mixture. The dark green band was collected and recrystallized from CH₂Cl₂/pyridine to yield 10.1 mg of **3** (84.7% yield).

Millimolar solutions of [(**tpfc**)Cr(III)(**py**)₂] for EPR measurements were freshly prepared in CH₂Cl₂–pyridine or CD₂Cl₂–pyridine-*d*₅ 10:1 mixtures (pyridine proportions higher than 10% were avoided because they produced larger spectral line widths). The solutions were frozen as quickly as possible in order to minimize [(**tpfc**)Cr(III)(**py**)₂] oxidation. A magnetically dilute sample of **3** was obtained by cocrystallization with the isomorphous complex [(**tpfc**)Co(III)(**py**)₂]¹³ in a 0.5:10 Cr(III)/Co(III) ratio. The cocrystals were transferred into a standard EPR tube and crushed with a long quartz rod to form a microcrystalline powder.

Compound **3** gave very fragile single crystals via recrystallization from benzene/*n*-heptane/pyridine. Diffraction data were obtained on a Nonius Kappa CCD diffractometer at low temperature (~110 K) to minimize atomic thermal displacements and increase signal-to-noise. The crystal structure was solved and refined by standard crystallographic techniques.

Crystal data for **3**: (C₄₇H₁₈CrF₁₅N₆)·1.5(C₆H₆), *M_r* = 1120.8, monoclinic, space group *C*2/*c* (No. 15), *a* = 40.705(1), *b* = 8.740(1), *c* = 26.999(2) Å, β = 98.19(1)°, *V* = 9507.2(12) Å³, *Z* = 8, ρ_{calcd} = 1.566 g cm^{–3}, 2θ_{max} = 50.8°, 7986 unique reflections. Final R1 = 0.093,

and wR2 = 0.152 for 3845 reflections with *F* > 4σ(*F*), wR2 = 0.216 for all data. The incorporated benzene solvent (one molecule in a general position and another located on inversion) is severely disordered in the lattice. The pentafluorophenyl substituent, located between the N22- and N23-pyrrole rings, also reveals excessively large thermal displacement parameters that reflect the partial disorder of this fragment.

[Cp₂Co][(**tpfc**)CrO] (**4**). A 25 mL two-neck flask was loaded under argon with **2** (16.1 mg, 18.7 μmol) and an excess of freshly sublimed cobaltocene; it was then evacuated. Vacuum transfer of acetone, followed by stirring for a few minutes (once the solvent had thawed) and solvent removal in vacuo yielded a residue that was redissolved in a minimum of CH₂Cl₂. Hexanes were added to precipitate a pink solid. The pink pellet obtained after centrifugation and supernatant removal was dried under vacuum to afford 15.7 mg of **4** (79.9% yield). UV–vis (CH₂Cl₂) λ_{max} [nm] (ε × 10^{–3} [M^{–1} cm^{–1}]): 432 (176.3), 542 (19.7), 578 (38.9). ¹H NMR (300 MHz) (CD₂Cl₂) δ in ppm: 9.13 (d, *J* = 4.0 Hz, pyrrole-H), 8.77 (d, *J* = 4.0 Hz, pyrrole-H), 8.72 (d, *J* = 4.7 Hz, pyrrole-H), 8.60 (d, *J* = 4.7 Hz, pyrrole-H). ¹⁹F NMR (282 MHz) (CD₂Cl₂) δ in ppm: –134.3 (m, 3F, *ortho*-F), –135.7 (m, 3F, *ortho*-F), –151.9 (m, 3F, *para*-F), –159.8 (m, 3F, *meta*-F), –160.2 (m, 3F, *meta*-F).

[(**tpfc**)Cr(OPPh₃)₂] (**5**). Solutions containing this air-sensitive compound were prepared as follows: a 1 mM solution of **2** in degassed toluene was allowed to react with 1 mM OPPh₃/1 mM PPh₃ for 30 min in the same solvent under argon. Alternatively, **5** was prepared by dissolving a small amount of **3** (to form a ~10 μM solution) in a degassed 1 mM OPPh₃ solution in toluene under argon. Ligand exchange was complete in 30 min.

[(**tpfc**)CrO] (**6**). This complex was prepared both by chemical and electrochemical oxidation of **2**. Chemical oxidation: excess dioxinium hexachloroantimonate was added to a CH₂Cl₂ solution of **2** cooled to –78 °C (dry ice/acetone); **6** was precipitated by adding cold hexanes. Electrochemical oxidation (for EPR): **2** (1–2 mg) was dissolved in 0.1 M tetrabutylammonium hexafluorophosphate/CH₂Cl₂ and oxidized at –78 °C (acetone/dry ice) in an electrochemical cell with platinum grid electrodes; the potential was scanned slowly (10 mV/s) from 0 to 1.5 V, and then a sample was transferred into an EPR tube, which was placed in liquid nitrogen.

Spectroscopy. UV–vis spectra were measured on a HP 8452 spectrophotometer. X-band EPR spectra were obtained on a Bruker EMX spectrometer equipped with a rectangular cavity working in the TE₁₀₂ mode. Variable temperature measurements were conducted with an Oxford continuous-flow helium cryostat (temperature range 3.8–300 K). Accurate frequency values were provided by a frequency counter built in the microwave bridge.

The absolute values of the [(**tpfc**)Cr(III)(**py**)₂] spin-Hamiltonian parameters were extracted from simulations of EPR spectra. Calculations were carried out on a PC using FORTRAN code¹⁴ based on

(13) Mahammed, A.; Giladi, I.; Goldberg, I.; Gross, Z. *Chem. Eur. J.*, in press.

Gladney's general EPR fitting program¹⁵ and adapted for simulations of EPR spectra of randomly oriented spin quartets. Transition fields and the corresponding average transition moments¹⁶ were computed in the magnetic field domain^{17,18} by matrix diagonalization of the $S = 3/2$ spin Hamiltonian:

$$\mathcal{H} = \beta(g_z H_z S_z + g_x H_x S_x + g_y H_y S_y) + D\left(S_z^2 - \frac{5}{4}\right) + E(S_x^2 - S_y^2)$$

D and E are defined in terms of the components of the diagonal fine-structure tensor as follows: $D_{zz} = (2/3)D$; $D_{xx} = (1/3)D + E$; $D_{yy} = (1/3)D - E$. In the absence of an applied magnetic field, the energy separation between the two Kramers doublets (zero-field splitting) is given by $2(D^2 + 3E^2)^{1/2}$. ⁵³Cr(III) hyperfine splitting (abundance 9.54%) and higher order terms were omitted in the spin Hamiltonian.

Electrochemistry. Voltammetric measurements were made on a CHI660 workstation with a normal three-electrode configuration, consisting of a glassy carbon electrode, an Ag/AgCl reference electrode, and a Pt-wire auxiliary electrode. Samples were in the millimolar range in 0.1 M [Bu₄N]PF₆/CH₂Cl₂ solution at room temperature. Spectroelectrochemical experiments were performed with the same solutions, but in a 0.1 mm path length cell using two gold minigrids as electrodes and a Ag/AgCl reference electrode.

Results and Discussion

We have shown previously that the reaction between **1** and chromium hexacarbonyl, followed by aerobic workup, affords the very stable Cr^{VO} corrole **2** in good chemical yields.³ This complex has been fully characterized by spectroscopic methods and X-ray crystallography. Our findings for **2** are similar to the observations of Matsuda et al. on a chromium complex of a different corrole,⁸ but they are in conflict with the report of a stable chromium(III) corrole¹⁰ (the latter work also was questioned in a review on metalcorroles¹¹). Matsuda also reported that a Cr^{VO} corrole can be oxidized to a state that was formulated as Cr^{VI} on the basis of UV-vis changes and the disappearance of the d¹ EPR signal. As this highly oxidized chromium corrole might also be a Cr^{VO} corrole radical, we decided to examine the properties of the product of one-electron oxidation of **2** as well as complexes in oxidation states lower than Cr^{VO}. First, we describe the electrochemistry of **2**, as its oxidation and reduction potentials are useful starting points for most of the syntheses.

Electrochemistry. The cyclic voltammogram of **2** displays two well-defined waves, separated by about 1.1 V (Figure 1, $E_{1/2}(\text{ox}) = 1.24$ V, $E_{1/2}(\text{red}) = 0.11$ V). Both processes are reversible, as demonstrated by the near unity ratio i_{pc}/i_{pa} as well as the linear dependence of the peak current on the square root of the scan rate. This indicates that relatively stable species have been formed.

The spectroelectrochemical results for **2** are shown in Figure 2. Upon oxidation at an applied potential of 1.64 V, the 402 nm absorption band (analogous to the Soret band in porphyrins) exhibits a large intensity reduction and shifts to 392 nm (Figure 2a). In addition, the band at 556 nm (analogous to the Q-band in porphyrins) disappears, and weak new bands appear at 650 nm. All these changes are normally associated with ligand oxidation; that is, they indicate that **2** is oxidized to [(tpfc[•])-Cr^{VO}]⁺ (**6**). Importantly, the spectrum of **2** is fully recovered upon reversal of the applied potential to about 1.0 V.

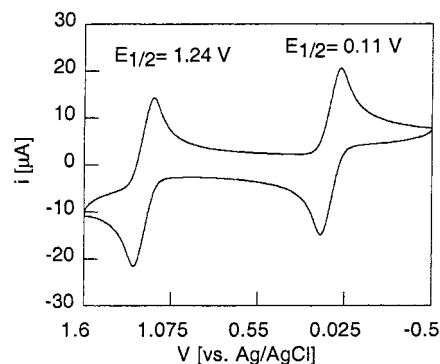


Figure 1. Cyclic voltammogram of **2** in 0.1 M TBAPF₆/CH₂Cl₂ solution (22 °C). Scan rate: 25 mV/s.

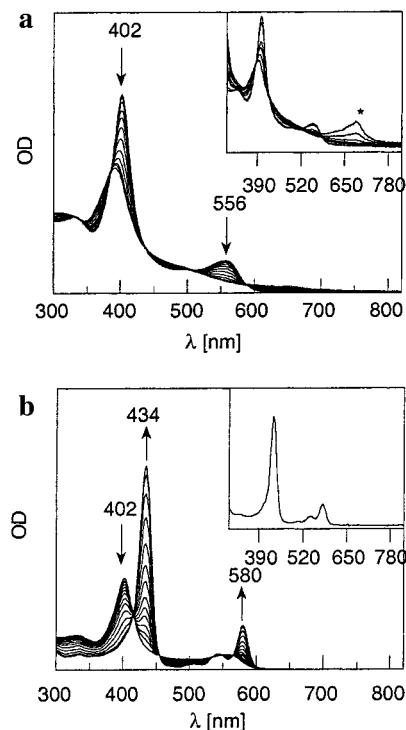


Figure 2. a. Spectroelectrochemical oxidation of a solution of **2** in 0.1 M TBAPF₆/CH₂Cl₂ at an applied potential of 1.64 V vs Ag/AgCl (22 °C). Inset: Spectral changes upon treatment of a CH₂Cl₂ solution of **2** with **7**. The marked band (*) is due to the excess organic radical present. b. Spectroelectrochemical reduction of a solution of **2** in 0.1 M TBAPF₆/CH₂Cl₂ at an applied potential of 0.0 V vs Ag/AgCl (22 °C). Inset: spectrum obtained after treatment of **2** with Cp₂Co.

The response to reduction is completely different (Figure 2b): the Soret band undergoes a very large increase in intensity and a 32 nm red shift from 402 to 434 nm; in addition, a sharp Q-band appears at 580 nm. The final spectrum is very similar to that of an (oxo)chromium(IV) porphyrin,¹⁹ thereby indicating that **2** is reduced at the metal to form [(tpfc)Cr^{IV}O]⁻ (**4**).

Our formulation of **4** as a Cr^{IV}O species accords with a literature report,⁹ but we differ in the assignment of the electronic structure of **6**. Thus, we decided to *isolate* the reduction and the oxidation products of **2** for further spectroscopic characterization, especially by EPR and NMR. For example, metal-centered oxidation of **2** would give a diamagnetic chromium(VI) corrole, that is, one that would be NMR-active and EPR-silent, whereas a radical formed by corrole oxidation would have very different properties.

(14) Bonomo, R. P.; Di Bilio, A. J.; Riggi, F. *Chem. Phys.* **1991**, *151*, 323.

(15) Swalen, J. D.; Gladney, H. M. *IBM J. Res. Dev.* **1964**, *8*, 515.

(16) van Veen, G. *J. Magn. Reson.* **1978**, *30*, 91.

(17) Asa, R.; Vännegård, T. *J. Magn. Reson.* **1975**, *19*, 308.

(18) Pilbrow, J. R. In *Transition Ion Electron Paramagnetic Resonance*; Clarendon Press: Oxford, 1990.

(19) Buchler, J. W.; Lay, K. L.; Castle, L.; Ullrich, V. *Inorg. Chem.* **1982**, *21*, 842.

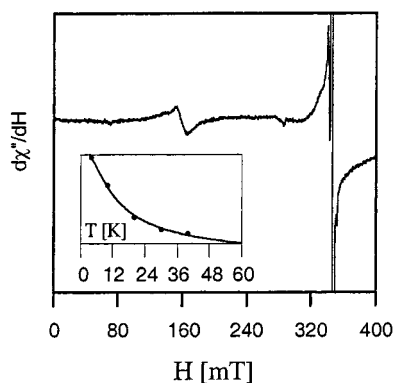
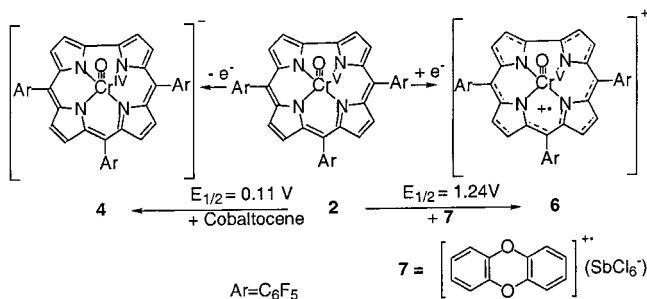


Figure 3. EPR spectrum of electrochemically generated **6** in 0.1 M TBAPF₆/CH₂Cl₂ frozen solution (30 K). Inset: total signal intensity vs temperature (the solid line was calculated for $\Delta E = 9 \text{ cm}^{-1}$).

Oxidation and Reduction Products of 2. The half-wave oxidation potential of **2** is 1.24 V: thus, for the preparation of **6**, we used the hexachloroantimonate salt of the cation radical of *p*-dibenzodioxin (**7**) (Scheme 2), a powerful oxidant ($E_{1/2}$

Scheme 2



$=1.41 \text{ V}$)¹² that does not interfere with NMR/EPR measurements. Compound **7** is a crystalline blue solid, stable at $-20 \text{ }^\circ\text{C}$ for weeks and of limited solubility in CH₂Cl₂. The last property is crucial for isolating the product without any paramagnetic impurity. Treating a micromolar solution of [(tpfc)-Cr^{VO}]/CH₂Cl₂ with aliquots of the oxidant in the same solvent results in the formation of a species with an electronic spectrum identical to the one seen in the electrochemical experiments (Figure 2a, inset). In sharp contrast to the characteristic room-temperature EPR spectrum of the d^1 Cr^{VO} complex **2**, that of **6** is only observable in frozen solutions and is very different (shown in Figure 3 for the electrochemically generated complex). Even though the region around $g \sim 2$ is obscured by the strong signal of **2**, the spectrum has a feature at half-field ($g \sim 4$) attributable to a spin-triplet species. This finding rules out metal oxidation (d^0 chromium(VI) would be diamagnetic and EPR-silent); indeed, this evidence strongly points to ligand oxidation.

The electronic structure of **6** is similar to that of peroxidase compound I, where a paramagnetic Fe^{IV}O (d^4) center is coupled to a porphyrin radical.^{20–22} Even more closely related is a V^{IV}O (d^1) porphyrin radical species.²³ In addition, there have been reports of oxidized corrole states in other complexes.^{7,24–29} The

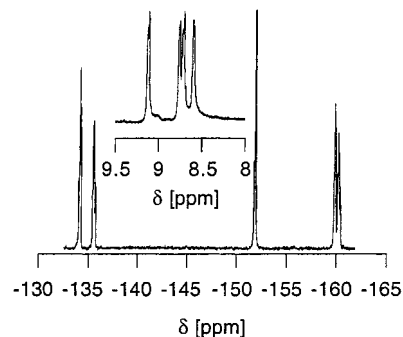


Figure 4. ¹⁹F and ¹H NMR (inset) spectra of [(tpfc)Cr^{VO}][−] (**4**) in acetone-*d*₆ solution (22 °C).

Cr^{VO} (d^1) and corrole radical electrons are coupled in **6** to give a triplet ground state, as the temperature-dependent EPR spectra confirm that $\Delta E[E(S=0) - E(S=1)]$ is positive (Figure 3, inset).³⁰ Analysis of the decrease in signal intensity with temperature from 4 to 40 K gives $\Delta E = 9 \text{ cm}^{-1}$.

Cobaltocene ($E_{1/2} = -0.83 \text{ V}$ vs Ag/AgCl)³¹ was chosen for the reduction of **2**, mainly because its oxidized form, cobaltocenium, is a nonnucleophilic counterion. The reaction proceeded smoothly on a semisynthetic scale, and **4** was isolated as a cobaltocenium salt (Scheme 2). Importantly, the absorption spectrum is virtually identical to the one obtained spectroelectrochemically (Figure 2b, inset). The ¹H NMR spectrum of **4** (Figure 4) clearly supports Cr^{VO} reduction. The β -pyrrole protons are not shifted from their diamagnetic position and are sharp; indeed, they display 4.0–4.7 Hz *J*-coupling constants, a very strong indication that **4** is diamagnetic. Owing to strong $\pi(\text{O})$ donation,³ a Cr^{IV} corrole is expected to have a (d_{xy})² ground state.^{32,33}

We conclude that reduction and oxidation of **2** are metal- and corrole-centered reactions, respectively. Complex **4** is a low-spin d^2 oxo corrole, analogous to Cr^{IV}O,³² Ru^{VI}O₂,³⁴ Mn^VN,^{35–38} and Mn^{VO} porphyrins and salens, and it is isoelectronic with the Mn^{VO} complex of **1**.⁴⁰

Chromium(III) Corroles 3 and 5. Cr^{VO} complexes of porphyrins and salens oxygenate olefins.^{41,42} The much less

- (20) Groves, J. T.; Haushalter, R. C.; Nakamura, M.; Nemo, T. E.; Evans, B. J. *J. Am. Chem. Soc.* **1981**, *103*, 2884.
 (21) Sono, M.; Roach, M. P.; Coulter, E. D.; Dawson, J. H. *Chem. Rev.* **1996**, *96*, 2841.
 (22) Green, M. T. *J. Am. Chem. Soc.* **2000**, *122*, 9495.
 (23) Schulz, C. E.; Song, H.; Lee, Y. J.; Mondal, J. U.; Mohanrao, K.; Reed, C. A.; Walker, F. A.; Scheidt, W. R. *J. Am. Chem. Soc.* **1994**, *116*, 7196.

- (24) Van Caemelbecke, E.; Will, S.; Autret, M.; Adamian, V. A.; Lex, J.; Gisselbrecht, J.-P.; Gross, M.; Vogel, E.; Kadish, K. M. *Inorg. Chem.* **1996**, *35*, 184.
 (25) Will, S.; Lex, J.; Vogel, E.; Adamian, V. A.; VanCaemelbecke, E.; Kadish, K. M. *Inorg. Chem.* **1996**, *35*, 5577.
 (26) Will, S.; Lex, J.; Vogel, E. H. S.; Gisselbrecht, J. P.; Hauptmann, C.; Bernard, M.; Gross, M. *Angew. Chem., Int. Ed.* **1997**, *36*, 357.
 (27) Kadish, K. M.; Adamian, V. A.; VanCaemelbecke, E.; Gueletti, E.; Will, S.; Erben, C.; Vogel, E. *J. Am. Chem. Soc.* **1998**, *120*, 11986.
 (28) Bendix, J.; Dmochowski, I. J.; Gray, H. B.; Mohammed, A.; Simkhovich, L.; Gross, Z. *Angew. Chem., Int. Ed.* **2000**, *39*, 4048.
 (29) Cai, S.; Walker, F. A.; Licocchia, S. *Inorg. Chem.* **2000**, *39*, 3466.
 (30) Abragam, A.; Bleaney, B. *Electron Paramagnetic Resonance Of Transition Ions*; Dover: New York, 1970.
 (31) Connelly, N. G.; Geiger, W. E. *Chem. Rev.* **1996**, *96*, 877.
 (32) Groves, J. T.; Kruper, J. W. J.; Haushalter, R. C.; Butler, W. M. *Inorg. Chem.* **1982**, *21*, 1363.
 (33) Nugent, W. A.; Mayer, J. M. *Metal-Ligand Multiple Bonds*; John Wiley & Sons: New York, 1988.
 (34) Groves, J. T.; Quinn, R. *Inorg. Chem.* **1984**, *23*, 3844.
 (35) Hill, C. L.; Hollander, F. J. *J. Am. Chem. Soc.* **1982**, *104*, 7318.
 (36) Buchler, J. W.; Dreher, C.; Lay, K.-L.; Lee, Y. J. A.; Scheidt, W. R. *Inorg. Chem.* **1983**, *22*, 888.
 (37) Groves, J. T.; Takahashi, T. *J. Am. Chem. Soc.* **1983**, *105*, 2073.
 (38) DuBois, J.; Hong, J.; Carreira, E. M.; Day, M. W. *J. Am. Chem. Soc.* **1996**, *118*, 915.
 (39) Groves, J. T.; Kruper, J. W. J. *J. Am. Chem. Soc.* **1980**, *102*, 6377.
 (40) Gross, Z.; Golubkov, G.; Simkhovich, L. *Angew. Chem., Int. Ed.* **2000**, *39*, 4045.
 (41) Groves, J. T.; Kruper, J. W. J. *J. Am. Chem. Soc.* **1979**, *101*, 7613.
 (42) Srinivasan, K.; Kochi, J. K. *Inorg. Chem.* **1985**, *24*, 4671.

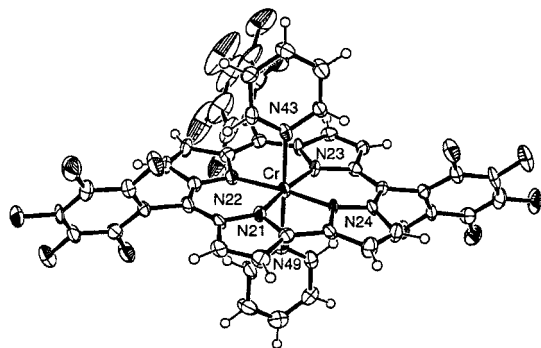


Figure 5. Molecular structure of **3**: the Cr–corrole core is flat, and the axial pyridines are nearly coplanar; Cr^{III}–N distances are 1.926(4)–1.952(4) Å (pyrrole) and 2.109(4)–2.129(4) Å (pyridine).

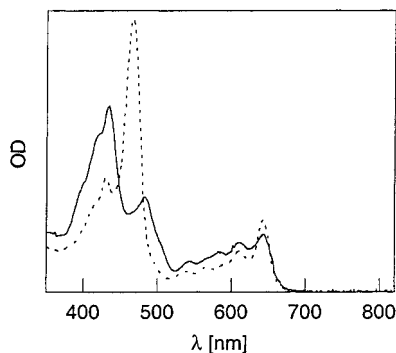


Figure 6. UV–vis spectra of [(tpfc)Cr(py)₂] (solid line) and [(tpfc)Cr(OPPh₃)₂] (dashed line) in toluene solution (22 °C).

Table 1. Selected Structural Parameters for Related [(tpfc)M^{III}(py)₂] Complexes (Diffraction Measurements at 110 K)

	[(tpfc)Cr(py) ₂]	[(tpfc)Fe(py) ₂]	[(tpfc)Co(py) ₂]
M–N(pyrrole) bond length range (Å)	1.926–1.952	1.865–1.923	1.873–1.900
M–N(pyridine) bond lengths (Å)	2.109, 2.129	2.028, 2.032	1.994, 1.994
N21···N23 (Å)	3.871	3.783	3.766
N22···N24 (Å)	3.860	3.770	3.775
axial-py twist angle (deg)	10.8	8.8	2.3

positive Cr^{VO}/Cr^{IVO} potential of **2** (0.11 V) relative to porphyrin and salen complexes (0.47–0.76 V)^{42,43} suggests that its reactivity will be much lower. This is indeed the case: **2** does not react with styrene, norbornene, or cyclooctene. Accordingly, we looked for a much stronger oxophile to reduce **2** to a chromium(III) corrole: treatment of **2** with triphenylphosphine produces very large absorption spectral changes with the final spectrum reminiscent of chromium(III) porphyrins.⁴⁴ Product **5** is [(tpfc)Cr(OPPh₃)₂], which is extremely air-sensitive and could not be isolated as a pure material; it was manipulated in solutions containing excess OPPh₃.

Substitution of the axial OPPh₃ in **5** was followed by changes in Soret absorption: upon addition of pyridine, **5** is converted to **3** (Figure 6).⁴⁵ The absence of isosbestic points indicates the

(43) Fujii, H.; Yoshimura, T.; Kamada, H. *Inorg. Chem.* **1997**, *36*, 1122.

(44) Summerville, D. A.; Jones, R. D.; Hoffman, B. M.; Basolo, F. *J. Am. Chem. Soc.* **1977**, *99*, 8195.

(45) Aliquots from a stock solution of **2** in toluene were injected into 2 mL toluene solutions that contained 10.6 mM OPPh₃, 0.9 mM PPh₃, and variable concentrations of pyridine (in the range 9.9–693 μM). In each case, the solution absorption spectrum was measured 15 min later to confirm that **2** was fully reduced and equilibrated with all potential ligands.

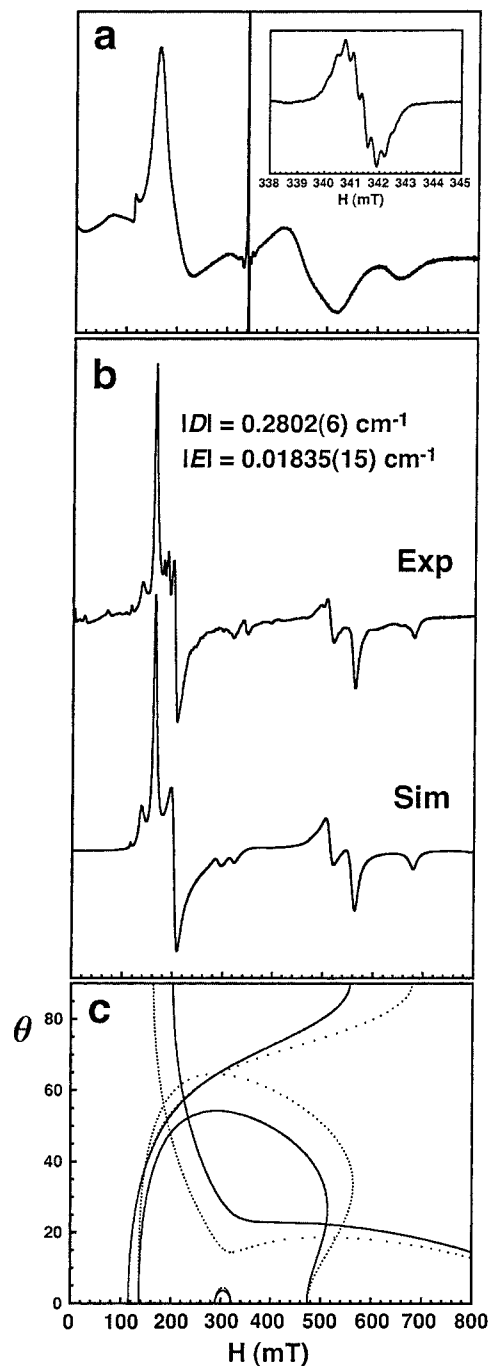


Figure 7. (a) Frozen solution EPR spectrum of [(tpfc)Cr(III)(py)₂] (solvent 10:1 CD₂Cl₂/pyridine-*d*₅, 77 K). Instrumental parameters: $\nu = 9.4878$ GHz, modulation frequency = 100 kHz, modulation amplitude = 12 G, microwave power = 8 mW, 10 scans. Sharp absorption at ~341.5 mT is assigned to Cr^{VO} (**2**) formed by oxidation of [(tpfc)Cr(III)(py)₂] in air. Resonance at high resolution (inset): nine-line multiplet is centered at $g \sim 1.985$ with a nitrogen superhyperfine coupling constant of $2.90(2) \times 10^{-4} \text{ cm}^{-1}$ (note that multiplet is not resolved in nondeuterated solvent).³ (b) Experimental vs computer simulated EPR spectra of a polycrystalline sample of [(tpfc)Cr(III)(py)₂] cocrystallized with [(tpfc)Co(III)(py)₂] (exptl, 3.9 K). Instrumental parameters: $\nu = 9.4795$ GHz, modulation frequency = 100 kHz, modulation amplitude = 10 G, microwave power = 6.4 mW, 15 scans. The features at ~180–190 mT are likely due to large crystallites (it proved difficult to produce a good powder with the limited amount of sample available); the weak feature at 342.5 mT and those below 100 mT are due to unknown impurities. Simulated spectrum computed with a Lorentzian function. (c) Relationship between the simulated spectrum and the angular dependence of the transition fields in the *D*-tensor reference frame: solid lines, angular dependence in *xz* plane ($\theta = 0 \rightarrow \pi/2$, $\phi = 0$); dotted lines, angular dependence in *zy* plane ($\theta = 0 \rightarrow \pi/2$, $\phi = \pi/2$).

presence of [(tpfc)Cr(OPPh₃)(py)] in appreciable amounts. Extracting equilibrium constants was not attempted, as such analysis is by no means trivial.⁴⁶ Qualitatively, the affinity of chromium(III) for pyridine is higher than for triphenylphosphine oxide.

It is apparent that **2** is obtained by air oxidation of Cr^{III} and that pyridine coordination inhibits this reaction. Accordingly, metal insertion into **1** was performed in pyridine, and the same solvent was utilized in all workup steps: **3** was obtained in good yield, and X-ray quality crystals were grown from a benzene/*n*-heptane/pyridine solution. Although the resolution was not very high, the basic structural aspects of this first authentic chromium(III) corrole were revealed; **3** features a flat corrole macrocycle and nearly coplanar mutual alignment of the two coordinated pyridines (Figure 5). The largest deviation from the mean plane defined by all the corrole atoms is only 0.14 Å. These features are very similar to those found in crystal structures of related bis-pyridine complexes of iron(III) and cobalt(III).^{7,13} Chromium(III) has a somewhat larger radius than the other two ions, yet it is still located perfectly in the plane defined by the four inner nitrogen atoms. This is accompanied, however, by a systematic increase in Cr–N compared to M–N distances in related complexes (Table 1). As observed for **2**,³ the bond distances between Cr and the corrole nitrogens are relatively short (1.92–1.94 Å) when compared to Cr^{II} porphyrins, which have M–N_{pyrrole} bonds in the range 2.012–2.141 Å.⁴⁷ Interestingly, the M–N_{pyridine} bonds are of similar lengths in both cases (2.026–2.121 Å).

Samples of compound **3** display rich EPR spectra, characteristic of chromium(III) complexes ($S = 3/2$) with a zero-field splitting similar in magnitude to the microwave quantum (at X band $h\nu \sim 0.3 \text{ cm}^{-1}$).⁴⁸ The EPR spectrum in frozen solution (Figure 7a) shows broad resonances at 3.8 K and above (spectral resolution in deuterated methylene chloride/pyridine is slightly improved relative to a nondeuterated solvent mixture). Thus, to extract the spin-Hamiltonian parameters of **3** reliably, we measured and simulated the EPR spectrum of a polycrystalline sample of [(tpfc)Cr(III)(py)₂] diluted in isomorphous [(tpfc)-

Co(III)(py)₂]¹³ (Figure 7b,c). We found a nearly isotropic g and a slightly rhombic fine-structure tensor: $g_z = 1.967(9)$, $g_x = g_y = 1.989(9)$, $|D| = 0.2802(6) \text{ cm}^{-1}$, $|E| = 0.01835(15) \text{ cm}^{-1}$, 4 K (these values change little in the range 4–150 K). The estimated zero-field splitting parameters for the compound in frozen solution are $|D| \sim 0.230(5) \text{ cm}^{-1}$ and $|E| \sim 0.02 \text{ cm}^{-1}$;⁴⁹ these values accord with those extracted from the solid-state experiment, indicating similar structures in both states. Importantly, the spin-Hamiltonian parameters of [(tpfc)Cr(III)(py)₂] are close to those reported for chromium(III) porphyrin species [(TPP)Cr(III)(Cl)(X)] (X = pyridine and other neutral N donors, $|D| \sim 0.156 \pm 0.012 \text{ cm}^{-1}$; X = neutral O- or S-donors, $|D| \sim 0.232 \pm 0.004 \text{ cm}^{-1}$; $|E| \leq 0.013 < 0 \text{ cm}^{-1}$) in frozen solution.⁴⁴

Concluding Remarks

We have successfully isolated and characterized chromium complexes of **1** in four different oxidation states. The one-electron oxidation and reduction reactions of **2** are corrole- and metal-centered (giving **6** and **4**, respectively), and oxygen-atom transfer from **2** to triphenylphosphine affords Cr^{III}, leading to the isolation of **5** and **3**. Aerobic oxidation of Cr^{III} corroles to Cr^{VO} species is reminiscent of the chemistry of chromium porphyrins (note the lower oxidation states relative to corroles),⁵⁰ wherein Cr^{II} complexes oxidize readily in aerobic environments to relatively inert Cr^{IV}O species. In experiments now underway, we are investigating whether it is possible to tune the reactivities of Cr^{VO} and Cr^{III} corroles to the point where both oxygen-atom transfer ($\text{Cr}^{\text{VO}} + \text{PPh}_3 \rightarrow \text{Cr}^{\text{III}} + \text{OPPh}_3$) and aerobic oxo regeneration ($\text{Cr}^{\text{III}} + 1/2\text{O}_2 \rightarrow \text{Cr}^{\text{VO}}$) are facile. Our goal is to elucidate the factors that control the rates of Cr^{VO} and Cr^{III} redox reactions in the hope that ultimately we will be able to design active catalysts for aerobic oxygenation of olefins and other hydrocarbons.

Acknowledgment. This work was supported by the NSF (H.B.G.), the Bayer Corporation, and the Israel Science Foundation (Z.G.).

Supporting Information Available: Tables of crystal data, structure refinement details, atomic coordinates, anisotropic thermal parameters, bond lengths, and bond angles for **3**. This material is available free of charge via the Internet at <http://pubs.acs.org>.

IC010723Z

(46) Sideris, E. E.; Valsami, G. N.; Koupparis, M. A.; Macheras, P. E. *Pharm. Res.* **1992**, *9*, 1568.

(47) Scheidt, W. R.; Brinegar, A. C.; Kimer, J. F.; Reed, C. A. *Inorg. Chem.* **1979**, *18*, 3610.

(48) Note that six-coordinate chromium(III) complexes are characterized by quasiisotropic g factors (<2) and zero-field splittings in the 0 to $\sim 2.5 \text{ cm}^{-1}$ range (McGarvey, B. R. In *Transition Metal Chemistry*; Carlin, R. L., Ed.; Dekker: New York, 1966; Vol. 3. Pedersen, E.; Toftlund, H. *Inorg. Chem.* **1974**, *13*, 1603. Bencini, A.; Gatteschi, D. In *Transition Metal Chemistry*; Nelson G. A., Figgis B. N., Eds.; Dekker: New York, 1982; Vol. 8, ref 43.).

(49) The relative intensities of some resonances in the frozen solution EPR spectrum were not reproduced well in the simulations. This is suggestive of D -tensor strain, which means that a distribution of spin-Hamiltonian parameters is needed to obtain a fit of the EPR line shape. Rotational freedom of the pyridine ligands is a probable cause of strain.

(50) Reed, C. A.; Kouba, J. K.; Grimes, C. J.; Cheung, S. K. *Inorg. Chem.* **1978**, *17*, 2666.